Supplementary Methods

Analysis of the Seasonality of SFTS Using Concentration Degree and Circular Distribution Methods

The circular distribution method is a statistical approach that transforms periodic data into linear data through trigonometric transformations. It can assess the presence of temporal clustering and even provide precise timing of peak occurrences. The central tendency is represented by the mean angle, while the dispersion is indicated by the standard deviation.

a. Concentration Degree Analysis

$$R_x = \frac{(r_3 + r_6 - r_9 - r_{12})}{2} + \frac{\sqrt{3}}{2} \cdot \big((r_5 + r_6 - r_9 - r_{10}) + (r_1 - r_4)\big)$$

$$R_y = \frac{(r_3 - r_6 - r_9 + r_{12})}{2} + \frac{\sqrt{3}}{2} \cdot \big((r_5 - r_6 - r_9 + r_{12}) + (r_1 - r_7)\big)$$

$$M = \sqrt{R_x^2 + R_y^2}$$

R_x and R_y represent dispersion, M represents concentration degree, and r_i represents the ratio of monthly incidence to the annual total, with subscripts indicating months.

When M =1， it indicates the maximum concentration, suggesting the disease occurred in only one month of the year. When M =0， it indicates minimum concentration, meaning the cases are evenly distributed throughout the 12 months. If M >0.90， it suggests strict seasonality. If M is between 0.70 and 0.90, it indicates strong seasonality. If M is between 0.50 and 0.70, it indicates moderate seasonality. If M is between 0.30 and 0.50, it indicates some seasonality. When M <0.30, the temporal distribution of cases is relatively uniform.

b. Circular Distribution Analysis

Cyclic statistics are used to evaluate peak periods and compare differences. A year of 365 days is converted to 360° , meaning 1 day is approximately 0.9863°. For simplicity, this is rounded so that 1 month corresponds to 30°. The middle day of each month is used as the group midpoint and converted to degrees: January is 15°, February is 45°, and so on.

① Calculation of Mean Angle and Standard Deviation

$$n = \sum f , X = \frac{1}{n}\sum f_i \cdot \cos a_i , Y = \frac{1}{n}\sum f_i \cdot \sin a_i , r = \sqrt{X^2 + Y^2},$$

$$\sin \bar{a} = \frac{Y}{r}, \cos \bar{a} = \frac{X}{r}, a_0 = \arctan\left(\frac{|X|}{|Y|}\right)$$

$$\bar{a} = \begin{cases} a_0 & X > 0, Y > 0 \\ 180° - a_0 & X < 0, Y > 0 \\ 180° + a_0 & X < 0, Y < 0 \\ 360° - a_0 & X > 0, Y < 0 \\ 90° & X = 0, Y > 0 \\ 270° & X = 0, Y < 0 \end{cases}$$

$$S = \frac{180°}{\pi}\sqrt{-2 \ln r}$$

f_i represents the frequency of a single sample, n represents the total number of observations, $a_i$represents the angle of a single sample, $\bar{a}$ represents the mean angle, which can be used to back−calculate the average onset day. $X$and Y represent the components used to determine the concentration trend of vector r along the horizontal and vertical axes. r represents the central tendency of the vector. The value of r is within the range [0,1] .If r=0, it indicates that there is no mean direction, meaning the average angle is undefined； the larger the value of r, the more concentrated the angles are；If r=1, it means all data points are concentrated in the same direction. Srepresents the index of angular dispersion, with a range from 0~∞，, also known as angular deviation. The peak onset period can be estimated by $\overline{a} \pm S$.

② Hypothesis Testing of Sample Mean Angle

Rayleigh's test is used, with the Rayleigh Z statistic.$Z = nr^2$。If $Z \geq 0.05$，, the mean angle is statistically significant.

Supplementary Tables

Supplementary Table 1 Analysis of Demographic Characteristics of SFTS Cases from 2019 to 2023

Year	2019		2020		2021		2022		2023		Total	
	Number of Cases	Proportion （%）	Number of Cases	Proportion （%）	Number of Cases	Proportion （%）	Number of Cases	Proportion （%）	Number of Cases	Proportion （%）	Number of Cases	Proportion （%）
Gender												
Female	238	53.72	342	53.35	277	51.01	453	53.86	799	56.47	2109	54.31
Male	205	46.28	299	46.65	266	48.99	388	46.14	616	43.53	1774	45.69
Total	443	100.00	641	100.00	543	100.00	841	100.00	1415	100.00	3883	100.00
Age												
0-10	0	0.00	2	0.31	2	0.37	1	0.12	0	0.00	5	0.13
10-20	1	0.23	1	0.16	0	0.00	0	0.00	3	0.21	5	0.13
20-30	4	0.90	10	1.56	1	0.18	9	1.07	7	0.49	31	0.80
30-40	13	2.93	14	2.18	11	2.03	17	2.02	27	1.91	82	2.11
40-50	41	9.26	56	8.74	36	6.63	63	7.49	66	4.66	262	6.75
50-60	91	20.54	142	22.15	128	23.57	204	24.26	284	20.07	849	21.86
60-70	167	37.70	194	30.27	157	28.91	243	28.89	369	26.08	1130	29.10
70-80	106	23.93	177	27.61	168	30.94	242	28.78	501	35.41	1194	30.75
80-90	20	4.51	45	7.02	39	7.18	62	7.37	145	10.25	311	8.01
90-100	0	0.00	0	0.00	1	0.18	0	0.00	13	0.92	14	0.36

Total	443	100.00	641	100.00	543	100.00	841	100.00	1415	100.00	3883	100.00
Occupation												
Farmer	352	79.46	560	87.36	457	84.16	724	86.09	1186	83.82	3279	84.45
Housework and Unemployed	48	10.84	31	4.84	44	8.10	71	8.44	147	10.39	341	8.78
Retired Personnel	20	4.51	17	2.65	18	3.31	25	2.97	39	2.76	119	3.06
Unknown	0	0.00	1	0.16	0	0.00	4	0.48	2	0.14	7	0.18
Nursery Workers and Nannies	0	0.00	0	0.00	0	0.00	1	0.12	0	0.00	1	0.03
Public Venue Attendant	0	0.00	0	0.00	1	0.18	0	0.00	0	0.00	1	0.03
Others	4	0.90	7	1.09	3	0.55	2	0.24	9	0.64	25	0.64
Medical Staff	1	0.23	3	0.47	0	0.00	1	0.12	0	0.00	5	0.13
Commercial Service	8	1.81	4	0.62	3	0.55	1	0.12	6	0.42	22	0.57
Student	1	0.23	2	0.31	1	0.18	1	0.12	4	0.28	9	0.23
Worker	7	1.58	9	1.40	11	2.03	9	1.07	12	0.85	48	1.24

Cadres and Staff	0	0.00	0	0.00	2	0.37	0	0.00	2	0.14	4	0.10
Preschool Child	0	0.00	1	0.16	0	0.00	0	0.00	0	0.00	1	0.03
Teacher	1	0.23	1	0.16	1	0.18	0	0.00	1	0.07	4	0.10
Non-institutionalized Child	0	0.00	1	0.16	1	0.18	1	0.12	0	0.00	3	0.08
Migrant Worker	1	0.23	1	0.16	1	0.18	1	0.12	5	0.35	9	0.23
Herder	0	0.00	2	0.31	0	0.00	0	0.00	2	0.14	4	0.10
Catering and Food Industry	0	0.00	1	0.16	0	0.00	0	0.00	0	0.00	1	0.03
Total	443	100.00	641	100.00	543	100.00	841	100.00	1415	100.00	3883	100.00

Table Notes: Data are presented as the number of cases and proportion (%). Age groups were categorized into 10-year intervals using a left-closed, right-open approach (e.g., [60,70) years, indicating individuals $\geqslant$60 and <70 years old)

Supplementary Table 2 Age Distribution of SFTS Cases (2019–2023)

Year	No. of cases (n)	Age (years), Median [Min–Max]	P^{a}
2019	443	65.0 [13.0–89.0]	
2020	641	66.0 [0.0–88.0]	
2021	543	67.0 [0.0–94.0]	< 0.001
2022	841	66.0 [2.0–89.0]	
2023	1415	69.0 [16.0–92.0]	
Comparison		P^{b}	Significance
2023 vs. 2022		3.90×10^{-7}	Yes
2023 vs. 2021		2.60×10^{-4}	Yes
2023 vs. 2020		2.92×10^{-8}	Yes
2023 vs. 2019		4.94×10^{-12}	Yes
2022 vs. 2021		5.12×10^{-1}	No
2022 vs. 2020		3.04×10^{-1}	No
2022 vs. 2019		5.84×10^{-3}	No
2021 vs. 2020		1.30×10^{-1}	No
2021 vs. 2019		1.69×10^{-3}	Yes
2020 vs. 2019		8.30×10^{-2}	No

Table Notes : *n* indicates the number of cases.

[a] The overall difference across years was assessed using the Kruskal-Wallis H test ($P = 6.26\times10^{-14}$). [b] Pairwise comparisons were performed using the Mann-Whitney U test.

All statistical tests were two-tailed. To account for multiple comparisons (10 pairs), a Bonferroni correction was applied, and the significance threshold was adjusted to α=0.005 (0.05/10). Exact P-values are provided for all comparisons.

Supplementary Table 3 Results of Concentration Degree and Circular Distribution of SFTS in Anhui Province (2019–2023)

Year	Concentration Degree (M)	Mean Angle $\bar{a}$ (°)	Std. Dev. (°)	Peak Day (MM-DD)	Peak Period (MM-DD)	Rayleigh Z	P
2019	0.49	180.20	68.76	07-02	04-23 to 09-10	104.95	2.63×10^{-46}
2020	0.61	167.80	57.00	06-19	04-22 to 08-16	238.26	3.37×10^{-104}
2021	0.50	176.81	66.59	06-29	04-22 to 09-04	140.69	7.93×10^{-62}
2022	0.60	162.62	57.57	06-14	04-17 to 08-12	306.41	8.49×10^{-134}

2023	0.53	174.42	64.49	06-26	04-22 to 08-31	398.66	7.30×10^{-174}

Table Notes: Seasonality of SFTS incidence was evaluated using circular distribution analysis. The concentration degree (M) and mean angle (a) were calculated to determine the strength and central timing of seasonal clustering, respectively. Rayleigh’s test (Z statistic) was applied to test the null hypothesis of a uniform circular distribution against the alternative of a preferred direction (seasonality). The Rayleigh test is inherently a one-sided test for circular uniformity. No adjustment for multiple comparisons was applied. $P < 0.05$ was considered statistically significant.

Supplementary Table 4 Regional Distribution of SFTS in Anhui Province (2019–2023)

City	Number of Cases	Annual Incidence (/100,000)	Deaths	Fatality Rate （%）
Chuzhou	1186	5.8765	9	0.7589
Ma’anshan	327	2.9861	29	8.8685
Lu’an	602	2.6970	26	4.3189
Anqing	469	2.2107	10	2.1322
Hefei	862	1.8282	31	3.5963
Chizhou	87	1.2873	0	0.0000
Tongling	73	1.0879	0	0.0000
Huangshan	67	1.0044	7	10.4478
Xuancheng	118	0.9399	6	5.0847
Wuhu	55	0.2961	3	5.4545
Huainan	19	0.1236	0	0.0000
Bozhou	13	0.0507	0	0.0000
Suzhou	3	0.0113	0	0.0000
Fuyang	2	0.0049	0	0.0000
Bengbu	0	0.0000	0	0.0000
Huaibei	0	0.0000	0	0.0000

Supplementary Table 5 Quantitative performance metrics for MMDM fitting across

Anhui Province and the five cities with the highest incidence rates from 2019 to 2023.

Region	Year	MSE	RMSE	R^2	P	MAE
Anhui	2023	126.4771	11.2462	0.7533	1.5149×10^{-13}	9.1203
Anhui	2022	75.3540	8.6807	0.7518	1.3808×10^{-16}	6.6896
Anhui	2021	28.6723	5.3547	0.6762	4.7014×10^{-11}	4.2174
Anhui	2020	34.5671	5.8794	0.7343	6.3845×10^{-12}	4.5124
Anhui	2019	21.8073	4.6698	0.65	9.6606×10^{-13}	3.4778
Anqing	2023	6.2806	2.5061	0.4036	5.0038×10^{-05}	1.734
Anqing	2022	3.2783	1.8106	0.5761	4.7425×10^{-07}	1.3476
Anqing	2021	2.3109	1.5202	0.218	6.0000×10^{-03}	1.1453
Anqing	2020	3.6064	1.8991	0.5507	7.4984×10^{-07}	1.3488
Anqing	2019	4.2093	2.0516	0.2027	2.6000×10^{-03}	1.4398
Chuzhou	2023	13.4682	3.6699	0.5931	3.0945×10^{-08}	2.8005
Chuzhou	2022	13.4512	3.6676	0.6522	4.4829×10^{-13}	2.7858
Chuzhou	2021	11.1183	3.3344	0.3878	6.0736×10^{-05}	2.6212
Chuzhou	2020	8.7796	2.963	0.3675	2.0000×10^{-04}	2.3792
Chuzhou	2019	2.2676	1.5058	0.5097	1.3997×10^{-06}	1.1458
Hefei	2023	17.3490	4.1652	0.5528	1.9500×10^{-07}	2.8642
Hefei	2022	7.5922	2.7554	0.5404	3.1011×10^{-07}	1.9978
Hefei	2021	4.8321	2.1982	0.3085	3.0000×10^{-04}	1.7529
Hefei	2020	2.6676	1.6333	0.5628	9.6350×10^{-08}	1.2628
Hefei	2019	2.3616	1.5367	0.1946	3.6000×10^{-03}	1.1082
Lu'an	2023	8.6658	2.9438	0.5337	3.9675×10^{-07}	2.0972

Lu'an	2022	4.2575	2.0634	0.432	5.9607×10^{-06}	1.47
Lu'an	2021	2.2641	1.5047	0.2003	2.5000×10^{-03}	1.2094
Lu'an	2020	2.8781	1.6965	0.3804	5.4946×10^{-05}	1.3476
Lu'an	2019	3.2344	1.7985	0.4423	1.2262×10^{-05}	1.3984
Ma'anshan	2023	2.2135	1.4878	0.5784	2.3274×10^{-08}	1.2566
Ma'anshan	2022	3.9523	1.988	0.5376	5.9188×10^{-06}	1.3542
Ma'anshan	2021	1.8192	1.3488	0.162	1.9500×10^{-02}	0.9948
Ma'anshan	2020	2.3401	1.5297	0.1814	2.6700×10^{-02}	1.149
Ma'anshan	2019	0.6256	0.791	0.1805	1.0000×10^{-02}	0.6059

Table Notes: Model performance was evaluated using multiple goodness-of-fit metrics, including Mean Squared Error (MSE), Root Mean Squared Error (RMSE), Mean Absolute Error (MAE), and the coefficient of determination (R2). Statistical significance of the Pearson correlation coefficients was assessed using two-sided tests. To account for multiple comparisons across 30 region-year combinations, Bonferroni correction was applied, and the adjusted significance threshold was set at α = 0.05/30 = 0.00167.

Supplementary Table 6 Model–estimated relative contributions of different transmission pathways in Anhui Province (2019–2023)

Pathway	Total contribution	Percentage (%)
Human-to-human	441.64	14.70%
Tick-mediated	1690.24	56.30%
Animal-related	872.27	29.00%
Total	3004.14	100.00%

Supplementary Table 7 Spatiotemporal variation in the relative importance of different transmission pathways across cities in Anhui Province (2019–2023)

Region	Year	Human (%)	Tick (%)	Animal (%)
Anhui	2019	13.19	69.58	17.23

Anhui	2020	15.58	54.10	30.32
Anhui	2021	14.46	50.09	35.45
Anhui	2022	19.47	67.41	13.13
Anhui	2023	23.66	56.12	20.21
Anqing	2019	11.48	62.52	26.01
Anqing	2020	12.27	56.84	30.89
Anqing	2021	4.94	39.20	55.86
Anqing	2022	6.49	38.38	55.13
Anqing	2023	6.67	40.95	52.38
Chuzhou	2019	5.53	42.18	52.29
Chuzhou	2020	13.54	33.97	52.49
Chuzhou	2021	7.80	48.23	43.97
Chuzhou	2022	9.75	72.05	18.20
Chuzhou	2023	10.62	52.30	37.08
Hefei	2019	5.20	39.82	54.98
Hefei	2020	8.97	42.98	48.05
Hefei	2021	8.82	38.38	52.80
Hefei	2022	11.53	38.94	49.53
Hefei	2023	15.70	43.53	40.77
Lu'an	2019	13.96	24.77	61.27
Lu'an	2020	6.53	48.76	44.71
Lu'an	2021	8.42	28.33	63.25
Lu'an	2022	6.47	48.67	44.86
Lu'an	2023	8.79	47.49	43.72
Ma'anshan	2019	4.10	27.95	67.95
Ma'anshan	2020	8.00	28.38	63.62
Ma'anshan	2021	6.42	27.72	65.86
Ma'anshan	2022	9.99	29.12	60.88
Ma'anshan	2023	11.06	36.47	52.47

Supplementary Figures

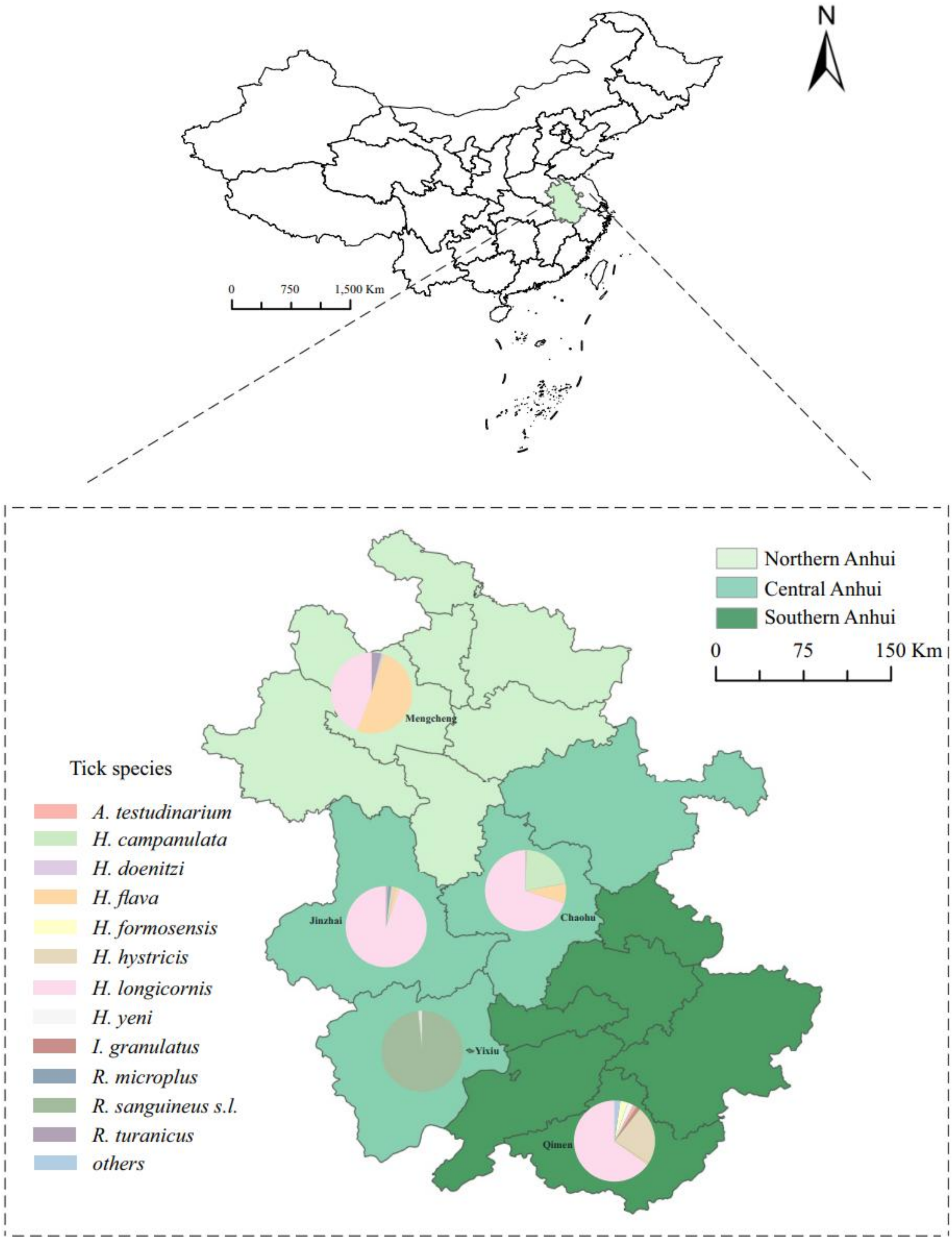

Supplementary Fig. 1. Tick species distribution in Anhui Province. The study area Anhui Province was divided into three regions, Northern Anhui (Suzhou, Huaibei, Bengbu, Bozhou, Fuyang, Huainan), Central Anhui (Hefei, Lu'an, Chuzhou, Anqing), and Southern Anhui (Tongling, Wuhu, Ma'anshan, Chizhou, Huangshan, Xuancheng). During the study period, a total of 1,480 ticks were collected from 5 counties/districts (Jinzhai County, Chaohu City, Qimen County, Yixiu District and Mengcheng County) in Anhui Province, with these specimens covering multiple tick species. Source data are provided as a Source Data file.

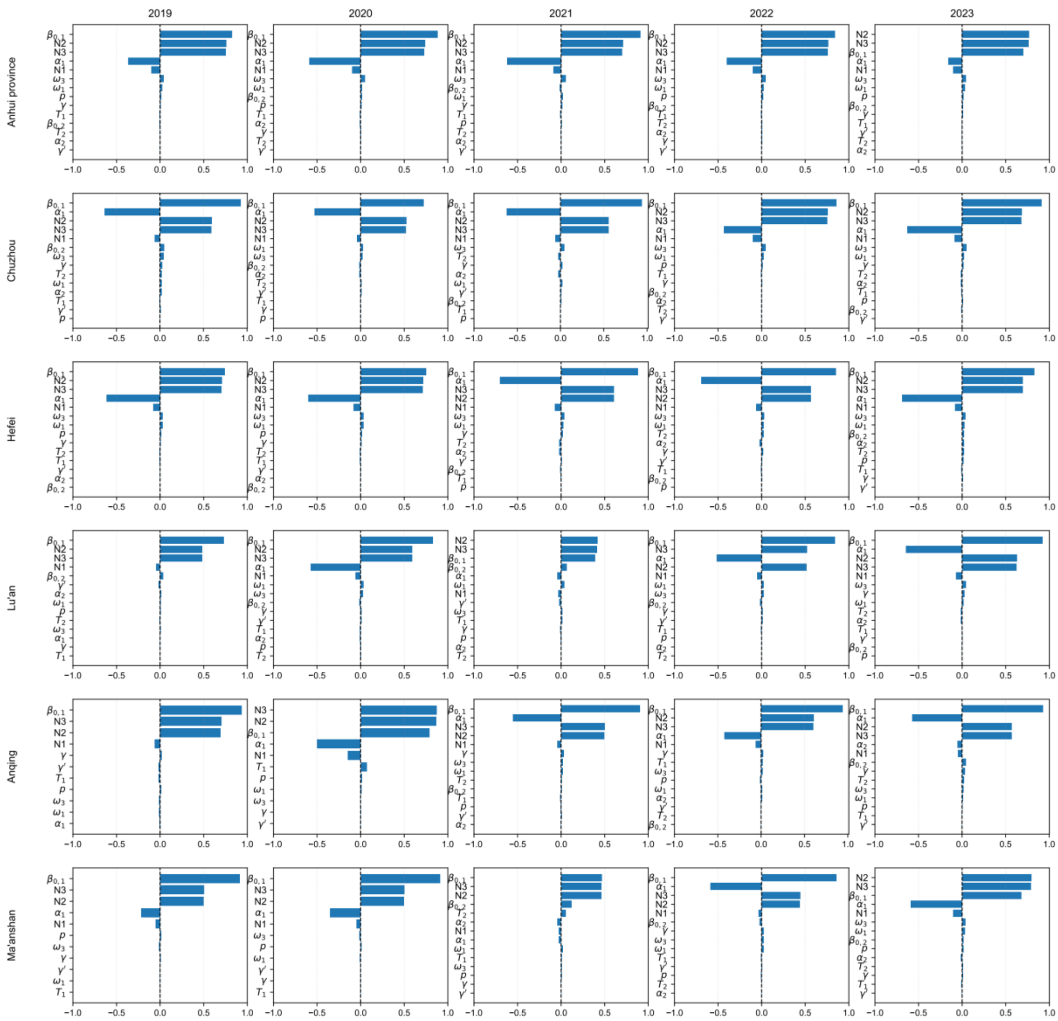

Supplementary Fig. 2. Global sensitivity of the basic reproduction number (R_0) to key model parameters based on PRCC, by region and year, Anhui Province. Source data are provided as a Source Data file.

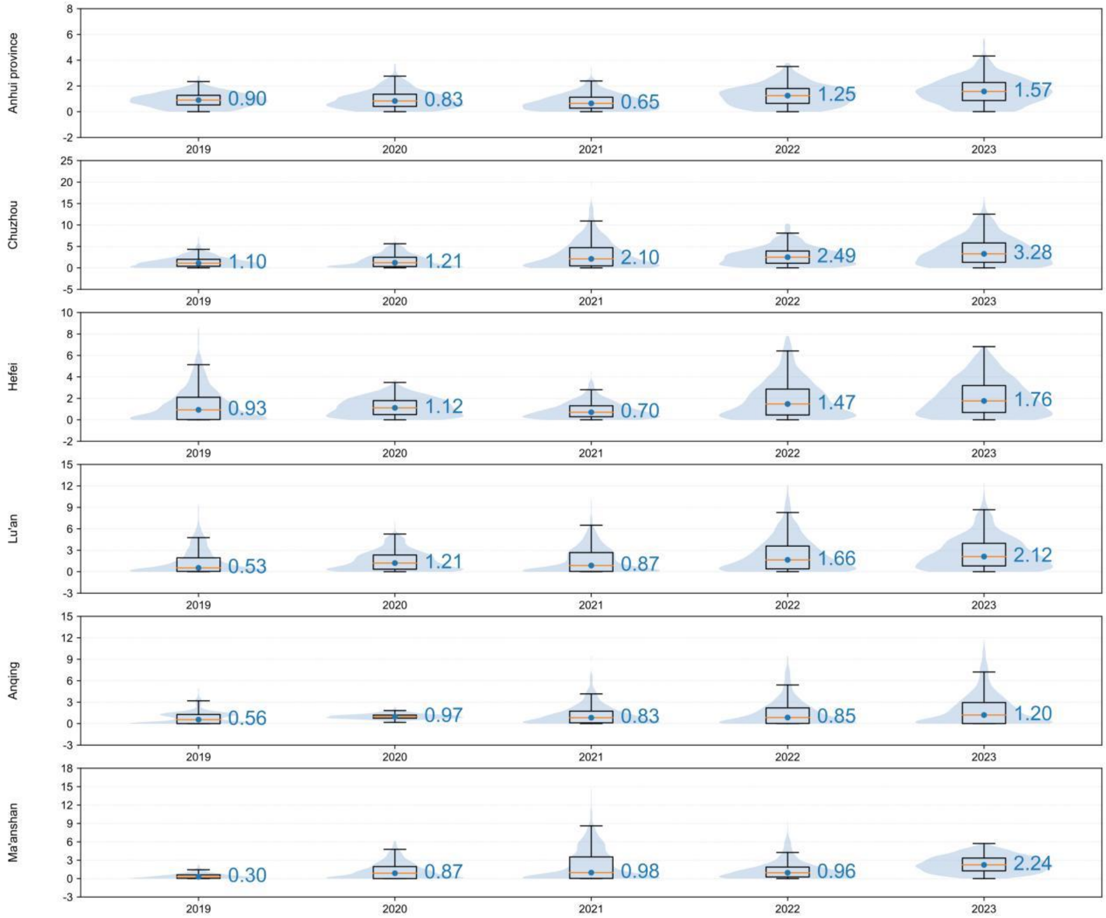

Supplementary Fig. 3. Probabilistic sensitivity analysis of the basic reproduction number for severe fever with thrombocytopenia syndrome in Anhui Province and the five high-incidence cities, 2019–2023. Probabilistic sensitivity analysis was performed using 5,000 Monte Carlo draws for each analysis. Source data are provided as a Source Data file.

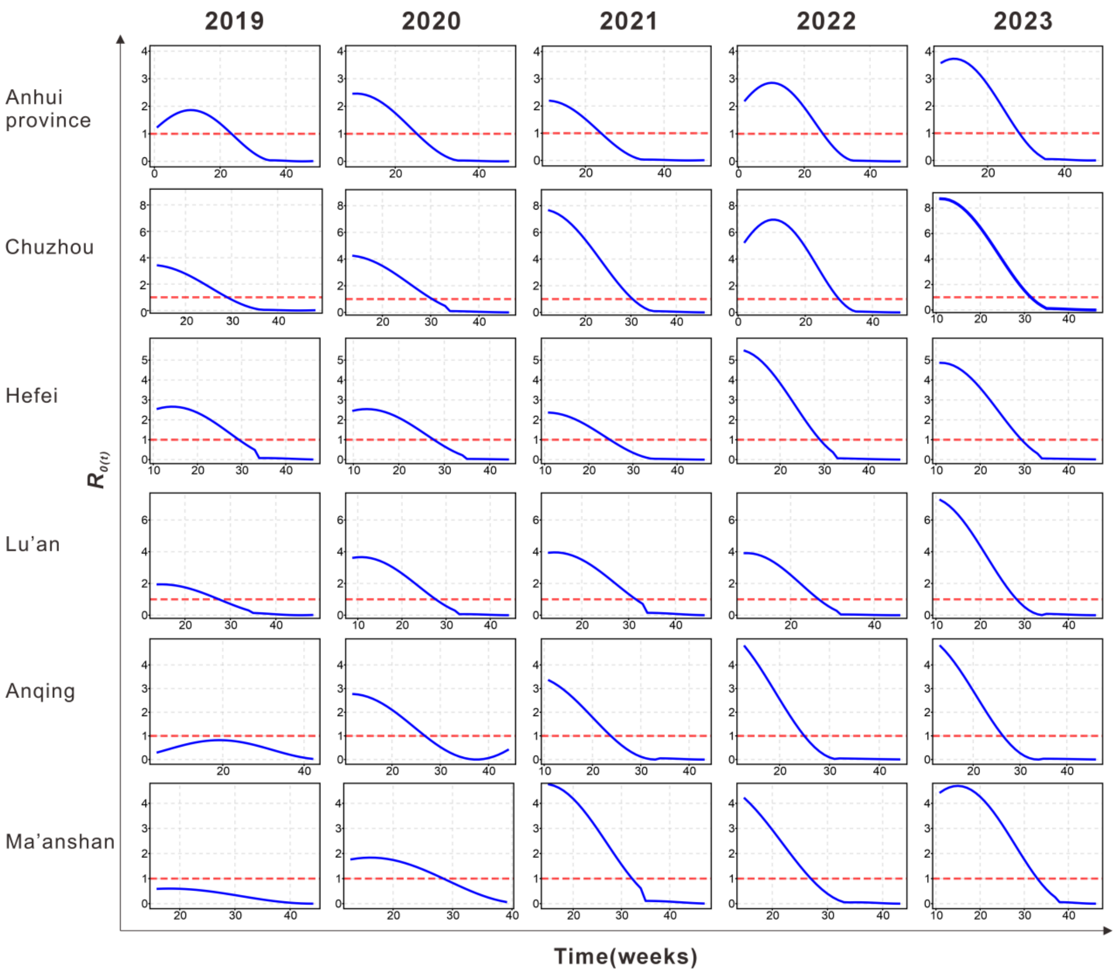

Supplementary Fig. 4. $R_{0(t)}$ Values of Anhui Province and the five cities with the highest incidence rates from 2019 to 2023. Source data are provided as a Source Data file.

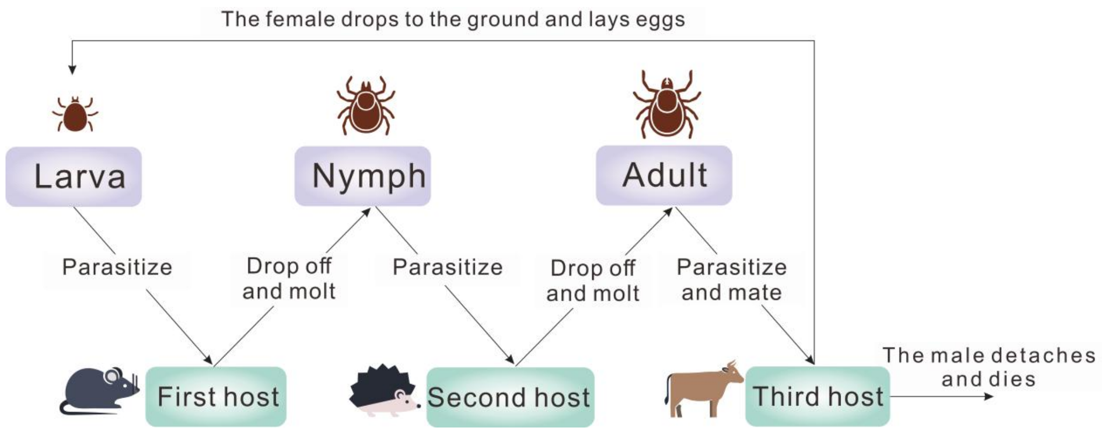

Supplementary Fig. 5. Life cycle of ticks highlighting the larval, nymphal, and adult blood-feeding stages. Larvae, nymphs, and adult ticks feed sequentially on first, second, and third hosts, with molting occurring after detachment between stages; adult females drop to the ground to lay eggs, completing the life cycle. The "first host", "second host", and "third host" represent generalized host categories across the tick's developmental blood-feeding sequence. The animals illustrated in the diagram are for conceptual visualization only and do not indicate specific or exclusive host species in this study.

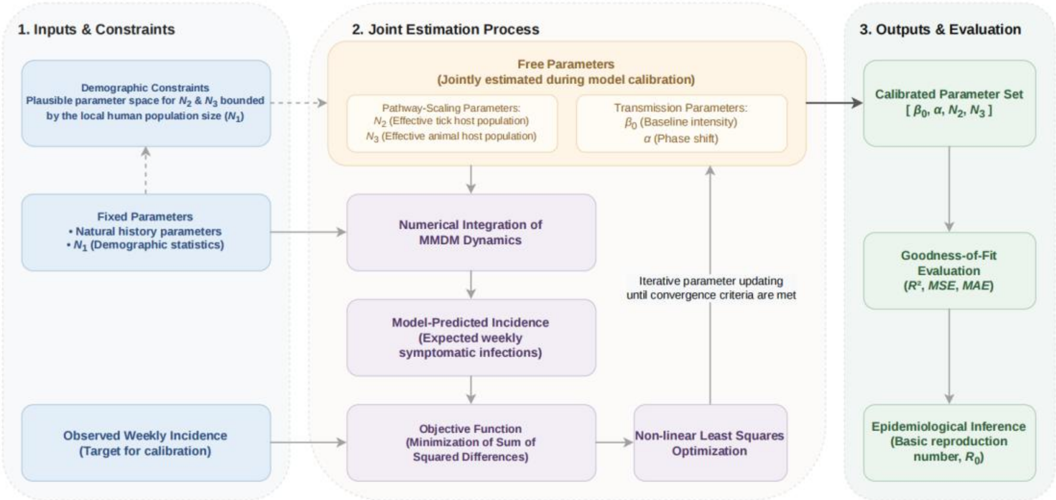

Supplementary Fig. 6. Workflow of joint parameter estimation and model calibration. Schematic of the joint parameter estimation framework. This flow diagram illustrates how the transmission parameters (β_0 , α) and the pathway-scaling parameters (N_2 , N_3) are treated as free parameters and jointly optimized. Notably, rather than fitting N_2 and N_3 in isolation or treating them as literal census counts, their plausible parameter space is explicitly bounded by the demographic constraint of the local human population size (N_1). This constraint ensures realistic effective contact intensities while avoiding implausible parameter combinations. The iterative non-linear least squares optimization loop minimizes the sum of squared differences between model-predicted incidence and observed data, ultimately yielding a stable and robust inference of the basic reproduction number (R_0). Specifically, for Anhui Province, both N_2 and N_3 were bounded between 10^3 and 10^6, whereas for the other five prefecture-level study areas, N_2 was bounded between 10^3 and 10^5 and N_3 between 10^3 and 10^4.